Binding of zebrafish lipovitellin and L1-ORF2 increases the accessibility of L1-ORF2 via interference with histone wrapping

NING JI[1*], CHONG-GUANG WU[1*], WEN-XIA WANG[1], XIAO-DIE WANG[1], YU ZHAI[2], LUQMAN ALI[1], ZHI-XUE SONG[1], GUOZHONG ZHANG[1], XU FENG[1], YU WANG[1], ZHAN-JUN LV[1] and XIUFANG WANG[1]

[1]Department of Genetics, Hebei Key Lab of Laboratory Animal Science, Hebei Medical University, Shijiazhuang, Hebei 050017, P.R. China; [2]Department of Basic Medicine, Hebei University of Chinese Medicine, Shijiazhuang, Hebei 050200, P.R. China

Received February 20, 2024; Accepted September 23, 2024

DOI: 10.3892/ijmm.2024.5443

Abstract. Long interspersed nuclear element-1 (L1) is highly expressed in the early embryos of humans, rodents and fish. To investigate the molecular mechanisms underlying high expression of L1 during early embryonic development, a C1-open reading frame (ORF)2 vector was constructed in which ORF2 of human L1 (L1-ORF2) was inserted into a pEGFP-C1 plasmid. C1-ORF2 vector was injected into early zebrafish embryos (EZEs) to observe expression of EGFP reporter protein by fluorescence microscopy. RNA-seq and RT-qPCR were used to detect the effects of lipovitellin (LV) on gene expression in EZEs. The binding ability of LV to L1-ORF2 DNA was detected by electrophoretic mobility-shift assay (EMSA). The chromatin recombinant DNase I digestion and ATAC-seq assay were used to evaluate the accessibility of plasmid DNA. C1-ORF2 vector induced high expression of enhanced green fluorescent protein (EGFP) reporter gene after it had been injected into 0 h post-fertilization (hpf) zebrafish embryos, although histone octamer inhibited expression of EGFP in C1-ORF2. SDS-PAGE was used to show that LV was the predominant protein binding ORF2 DNA in 0 hpf zebrafish embryo lysate (ZEL). Both ZEL and purified LV from ZEL attenuated the inhibitory effects induced by histone. LV bound histone to interfere with the binding of histone to ORF2 DNA. Both *in vitro* chromatin reconstitution experiments and assay for transposase-accessible chromatin with sequencing with HeLa cells were utilized to demonstrate that the interference induced by LV resulted in increased accessibility of C1-ORF2. Transcription experiments *in vitro* verified that LV could enhance the mRNA levels of zebrafish early embryo expression genes grainyhead-like transcription factor 3 (GRHL3), SRY-box transcription factor 19a (SOX19A) and nanor (NNR) and also of the EGFP gene. LV was found to increase the expression levels of the zebrafish early embryo expression genes in liver tissue after LV had been injected into the abdominal cavity of adult male zebrafish. Taken together, the findings of the present study demonstrated that LV activates the expression of EGFP induced by ORF2 in EZEs by enhancing the accessibility of ORF2 DNA.

Introduction

Long interspersed nuclear element-1 (L1) is a transposable element in vertebrate genomes, including zebrafish, frogs and humans (1-4). Human and zebrafish L1 exhibit 70% homology and both human and zebrafish L1 contain two open reading frames (ORFs), ORF1 and ORF2 (3,5). ORF2-encoded protein is evolutionarily conserved between zebrafish and humans, containing both endonuclease and reverse transcriptase, whereas no conserved domains are found in ORF1-encoded protein (6-8). L1 is silenced in differentiated cells to prevent uncontrolled mutagenesis (9). L1 is highly expressed in early embryos of humans, rodents and fish (9-12). L1 elements exhibit active expression prior to the 8-cell stage, which is subsequently decreased in blastocysts during human embryo development. The expression of zebrafish L1 is increased during the stage of 50% epiboly [5.25 h post-fertilization (hpf)], although the expression was reduced from the 4-somite (11 hpf) stage onwards (10,11). L1 serves a crucial role in early embryonic development; inhibition of L1 transcription has been suggested to impede embryo development in mice (1). Although numerous studies have reported the processes associated with L1 activation during early embryonic development, the underlying molecular mechanisms that regulate L1 transcription have yet to be fully elucidated (10,11).

Lipovitellin (LV), constituting the majority of vitellogenin, is an energy 'reservoir' that is gradually used during embryonic development (13,14). Additionally, LV has antioxidant activity and contributes to immune defense functions (15). However,

Correspondence to: Professor Zhan-Jun Lv or Professor Xiufang Wang, Department of Genetics, Hebei Key Lab of Laboratory Animal Science, Hebei Medical University, 361 East Zhongshan Road, Shijiazhuang, Hebei 050017, P.R. China
E-mail: lslab@hebmu.edu.cn
E-mail: wangxf1966@hebmu.edu.cn

*Contributed equally

Key words: long interspersed nuclear element, zebrafish embryo, lipovitellin, open reading frame 2, chromatin reconstitution

whether LV serves a key role in the high expression of L1 in early zebrafish embryos (EZEs) has been unclear.

The present study aimed to elucidate the mechanisms by which LV increasing the expression of EGFP gene induced by L1-ORF2 (ORF2) and EZE expression genes, which is related with the ability of LV binding with ORF2 DNA and increasing chromatin accessibility.

Materials and methods

Plasmid construction. The expression vectors C1-ORF2, C1-Alux14 and C1-LacZ were constructed as previously described (16). C1-delPolyA vector was obtained by deleting the poly(A) DNA sequence (240 bp) from the C1-ORF2 vector using the *Mlu*I and *Apa*I restriction enzymes.

ZE and plasmid microinjection. TU strain zebrafish were purchased from Nanjing Yaoshunyu Biotechnology Co., Ltd. and maintained under a 14/10-h light/dark cycle at 28.0±0.5˚C, as previously described (17,18). Experimental procedures were approved by the Institutional Animal Care and Use Committee of Hebei Medical University (approval no. IACUC-Hebmu-2021009). Adult fish were fed twice a day. A total of 10 pairs of adult male and female (>16 weeks) zebrafish (weight, 0.36-0.44 g) were maintained at 28˚C and the embryos were obtained from breeding pairs at 8-9 a.m. Fertilized embryos collected within 45 min (1-cell stage embryos) were considered 0 hpf zebrafish embryos (ZEs). Spawns for which the survival rate of the normal embryos up to 24 h was >90% were considered good-quality embryos, whereas survival rate of the normal embryos up to 24 h was <30% was considered to contain poor-quality embryos.

The plasmids were diluted into a buffer of 0.1 mol/l NaCl and 10 mmol/l Tris-HCl (pH 7.2); final concentration of plasmids was 0.1 μg/μl. A total of 1.7 nl plasmid solution was microinjected into ZE animal pole or yolk sac and the embryos were then cultured in a Petri dish to 6, 12, 24, 48 or 72 h at 28˚C.

The expression of the EGFP reporter protein in ZEs was observed under a fluorescence microscope (Leica Microsystems GmbH) in 40X at an excitation wavelength of 490 nm. ImageJ software 1.53 (National Institutes of Health) was used to analyze the fluorescence intensity.

Preparation of ZE lysate (ZEL) and LV protein purification. The 0 hpf ZEs were collected and 10X embryo buffer was added to the 0 hpf ZEs at a concentration of 1X (0.1 mol/l NaCl, 0.5 mmol/l PMSF, 2 mmol/l dithiothreitol, 0.5 mmol/l EDTA and 10 mmol/l Tris-HCl, pH 7.4). The embryos were crushed using an ultrasonic cell processor (VIBRA-Cell™ Sonics VCX105; Sonics & Materials, Inc.). The homogenized embryos were centrifuged at 13,400 g for 5 min at 4˚C and supernatant (ZEL) was collected. The optimal density (OD) was measured by ultraviolet spectrophotometer (UV-2800A; UNICO Instrument Co., Ltd. Shanghai) at 280 nm and the ZEL was subsequently diluted using 1X embryo buffer (0.475, 0.95, 1.90, 3.80 and 7.60 μg/μl).

LV was purified from ZEL as previously described (19). Purified LV was analyzed using Easy-nLC1200 high-performance liquid chromatography (HPLC; Shanghai Luming Biotechnology Co., Ltd.). The purified LV was labeled using fluorescein isothiocyanate (FITC), as described by Li *et al* (20). Aliquots of 1.7 nl FITC-LV (20 μg/μl) were injected into the animal pole or yolk sac of 0 hpf or 3 hpf ZEs under the stereomicroscope and fluorescence was observed at 72 h after injection. Male zebrafish plasma (MZP) was isolated as described by Medina-Gali *et al* (21). Globin was extracted from MZP using a Micro Protein PAGE Recovery kit [Real-Times (Beijing) Biotechnology Co., Ltd.] and identified by SDS-PAGE (15% gel), as previously described (22).

In vitro chromatin reconstitution. A total of two chromatin reconstitution methods were used: Incubation reconstitution, as described by Stein *et al* (23), and the salt-dialysis reconstitution method described by Lusser and Kadonaga (24).

In incubation reconstitution process (7,25), plasmids were diluted into plasmid solution to a final concentration of 0.1 μg/μl. Each plasmid was incubated with histone octamer (0.000, 0.005, 0.010, 0.020, 0.040, 0.080 and 0.160 μg/μl) and LV (0.000, 0.625, 1.250, 2.500, 5.000 and 10.000 μg/μl) or BSA (0.000, 0.625, 1.250, 2.500 and 5.000 μg/μl) (Yuanye Biotechnology Co., Ltd.) in buffer comprising 0.1 mol/l NaCl and 10 mmol/l Tris-HCl at room temperature for 30 min.

In the salt-dialysis reconstitution (24), each plasmid (at a final concentration of 0.1 μg/μl) was mixed with histone octamer and LV (or BSA) in initial buffer containing 2 mol/l NaCl, 1 mmol/l EDTA and 10 mmol/l Tris-HCl (pH 7.2). The chromatin was placed into a dialysis bag (0.5 kDa; Beijing Solarbio Science & Technology Co., Ltd.) for 4 h dialysis at 8˚C. Finally, the volume of the reconstituted chromatin was adjusted to 0.4 ml using buffer containing 0.1 mol/l NaCl and 10 mmol/l Tris-HCl (pH 7.2).

SDS-PAGE. The samples loaded were as follows: Sample 1, 75 μl 1 mg/ml salmon sperm DNA (Beijing Solarbio Science & Technology Co., Ltd.) was incubated with 75 μl ZEL (57 mg/ml) at 4˚C for 15 min, and centrifuged for 5 min at 13,400 g at 4˚C. For sample 2, the supernatant of sample 1 was incubated with 7.5 μl 10 mg/ml salmon sperm DNA at 4˚C for 15 min, then centrifuged for 5 min at 13,400 g at 4˚C. Samples 3 and 4 were obtained via repeating this procedure. The samples were added to 40 μl Tris-HCl containing 10 μl 10% SDS and 10 μl loading buffer. Sample 5 contained 8 μl supernatant from the fourth salmon-sperm DNA precipitate mixed with 8 μl Tris-HCl, 4 μl 10% SDS and 4 μl loading buffer. Sample 6 comprised 4 μl ZEL mixed with 12 μl Tris-HCl, 4 μl 10% SDS and 4 μl loading buffer. For sample 7, 75 μl 1 mg/ml salmon-sperm DNA was mixed with 75 μl ZEL (57 mg/ml); 750 μl 0.075 mol/l NaCl was then added and the mixture was incubated at 4˚C for 15 min and centrifuged for 5 min at 13,400 g. The precipitate was dissolved in 40 μl Tris-HCl containing 10 μl 10% SDS and 10 μl loading buffer. Sample 9 (histone) was prepared in the same way as sample 7 (histone) above. To generate sample 10, 175 μl FCS was incubated with 75 μl 1 mg/ml salmon-sperm DNA at 4˚C for 15 min and centrifuged for 5 min at 13,400 g. This precipitate was dissolved in 40 μl Tris-HCl containing 10 μl 10% SDS and 10 μl loading buffer. Sample 11 was generated by mixing 4 μl FCS with 12 μl Tris-HCl containing 4 μl 10% SDS and 4 μl loading buffer. All samples were boiled at 100˚C for 2 min.

A total of 5 μl each sample was loaded onto each lane and subjected to SDS-PAGE (15% gels).

Establishment of in vitro transcription system. Nuclear Extraction kit (Beyotime Institute of Biotechnology) was used to extract nuclei from 20 hpf ZEs using 0.42 mol/l NaCl for two sequential extractions. Each 1 ml supernatant was mixed with 330 mg ammonium sulfate, centrifuged at 13,400 g for 5 min at 4˚C and the resulting precipitate was dissolved in 0.5X Tris-EDTA (TE) buffer (10 mmol/l Tris, 1 mmol/l EDTA, pH 8.0) and loaded onto an equilibrated Sephadex G50 column (1.5x20 cm height, Pharmacia) to obtain crude RNA polymerase II for use in the following experiments.

In vitro transcription of chromatin was performed as described by You *et al* (26). Chromatin from deyolked 3 hpf ZEs (1,000 cells) was extracted as described by Purushothaman *et al* (27). The chromatin was dissolved in buffer at 4˚C (0.1 mol/l NaCl and 10 mmol/l Tris-HCl; pH 7.2).

A total of 10 nmol/l C1-ORF2 recombinant (or chromatin) was incubated for 1 h at 30˚C in reaction buffer with crude RNA polymerase II for 1 h at 30˚C in 400 mmol/l Tris-HCl reaction buffer, which includes 200 μmol/l nucleotides, 20 U RNase inhibitor, 200 mmol/l $MgCl_2$, 25 mmol/l tris (2-carboxyethyl) phosphine and 20 mmol/l spermidine.

The reaction was terminated by adding 125 mmol/l Tris-HCl (pH 7.5) containing 12.5 mmol/l EDTA, 150 mmol/l NaCl, 1% SDS and 2 μg/μl protease K at 55˚C for 1 h. Reverse transcription-quantitative (RT-q)PCR analysis was used to detect the mRNA levels of EZE expression genes as previously described (28). Table I shows primers for RT-qPCR analysis.

RT-qPCR and RNA sequencing (RNA-seq). Aliquots of 20 μl LV (50 μg/μl) were injected into the abdominal cavity of adult male zebrafish (weight, 0.37-0.43 g). Total RNA was extracted from zebrafish livers 24 h after the zebrafish had been fed at 28˚C in a flowthrough system. The zebrafish were submersed in water containing 100 mg/l 3-aminobenzoate methanesulfonate (Beijing Mreda Technology, Inc.) for anesthesia. The zebrafish enterocoelia were opened to obtain the zebrafish liver. Total RNA was extracted using TRIzol® (Thermo Fisher Scientific, Inc.) from liver tissues. Total RNA was reverse-transcribed into cDNA using RevertAid First Strand cDNA Synthesis kit (Thermo Fisher Scientific, Inc.) according to the manufacturer's protocol. Expression levels of the EZE expression genes GRHL3 (grainyhead-like transcription factor 3), SOX19A (SRY-box transcription factor 19a) and NNR (nanor) were detected using qPCR kit (cat. no. QP031, GeneCopoeia). qPCR was performed using the following thermocycling conditions: Initial denaturation at 95˚C for 2 min, followed by 40 cycles at 95˚C for 10 sec and 56˚C for 40 sec. The $2^{-\Delta\Delta Cq}$ method was used to calculate the relative mRNA expression levels (29). The primer pairs utilized for RT-qPCR analysis are shown in Table I.

Zebrafish were placed into water containing 0.5 g/l 3-aminobenzoate methanesulfonate for ≥20 min to ensure death, prior to storage at -20˚C.

RNA-seq analysis was performed by Shanghai OE Biotech. Co., Ltd., as previously reported (28). Total RNA was extracted from zebrafish liver tissue using TRIzol®. The purity and quantification of the RNA was evaluated using a NanoDrop™ 2000 spectrophotometer (Thermo Fisher Scientific, Inc.), whereas RNA integrity was assessed using Agilent 2100 Bioanalyzer (Agilent Technologies, Inc.). Subsequently, the libraries were constructed using a TruSeq® Stranded mRNA LT Sample Prep kit (cat. no. NR616-02, Illumina, Inc.). Gene Ontology (GO; geneontology.org/) enrichment analysis were performed.

Electrophoretic mobility-shift assay (EMSA). Fragments were obtained by digesting C1-ORF2 (*Xho*I/*Pst*I), C1-Alux14 (*Hin*dIII/*Nhe*I), C1-LacZ (*Apa*I/*Xho*I) and C1 (*Xho*I/*Pst*I). These fragments were precipitated with ethanol, centrifuged at 13,400 g for 5 min at 4˚C and precipitate was dissolved in double distilled water. All restriction enzymes were purchased from Takara Biotechnology Co., Ltd. The final concentration of fragments was 20 ng/μl and the concentration determination method was measured by ultraviolet spectrophotometer (UV-2800A; UNICO Instrument Co., Ltd. Shanghai) at 280 nm; these fragments were incubated with histone or LV for 15 min at room temperature in 10 mmol/l Tris-100 mmol/l NaCl buffer. LV concentrations were 0.0000, 0.0625, 0.1250, 0.2500, 0.5000, 0.7500, 1.0000, 1.2500, 1.5000 and 1.7500 μg/μl in the experiments that ORF2, Alux14, C1 fragments were incubated with LV. The LV concentrations were 0.0000, 0.0125, 0.0625 and 0.3125 μg/μl and histone concentrations were 0.025 μg/μl in the experiments of the effects of incubation order. The LV concentrations were 0.0000, 0.0625, 0.1250, 0.2500, 0.5000, 1.0000 and 2.0000 μg/μl, the histone concentrations were 0.015, 0.020, 0.025, 0.030 μg/μl to assess effects of histone concentrations. A total of 10 μl of each sample was loaded into a well with the gel; all experiments were using 1.5% agarose gel with 5% ethidium bromide (cat. no.1239-45-8; Shanghai Yien Chemical Technology Co., Ltd.). Finally, images were captured using an Alpha Innotech gel-imaging analyzer (Alpha Innotech Corporation).

Chromatin immunoprecipitation (ChIP)-PCR assay. ChIP assay was employed to validate the affinity of LV with ORF2. ZEs (25 mg, 0 hpf) were microinjected using C1-ORF2 or C1-Alux14 (control) plasmids. Subsequently, the injected embryos were incubated at 28˚C for 2 h and frozen at -20˚C for processing. Samples were prepared using the SimpleChIP® Plus Enzymatic chromatin IP kit (Cell Signaling Technology, Inc.; cat no. #9005), following the manufacturer's protocol. A total of 1.5% formaldehyde was added into the embryos for 30 min at room temperature to produce cross-linked protein and DNA and then chromatin fragments were obtained using sonication (20 sec per time; 800 Hz) at intervals of 30 sec (20 cycles) at 4˚C, followed by centrifugation at 13,400 x g for 5 min at 4˚C. The chromatin fragments were incubated with 0.03 μg/μl anti-LV antibody at 4˚C for overnight. PCR was performed using the following EGFP primers: Forward, 5'-ACATCCTGGGGCACAAGC-3' and reverse, 5'-CTTGTACAGCTCGTCCATGC-3'. PCR kit [cat. no. ET101, TIANGEN BIOTECH (BEIJING) CO., LTD.] was performed using the following thermocycling conditions: Initial denaturation at 94˚C for 3 min, followed by 30 cycles of 94˚C for 30 sec, 55˚C for 30 sec and 72˚C for 60 sec and final extension at 72˚C for 5 min. PCR products (311 bp) were separated by 1% agarose gels and visualized using a UV transilluminator (Alpha Innotech Corp. USA).

Table I. Primers used for reverse transcription-quantitative PCR.

Target	Sequence, 5'→3'	Length of product, bp
EGFP	Forward: GCACCATCTTCTTCAAGGAC	
	Reverse: TTGTCGGCCATGATATAGAC	181
GRHL3	Forward: AGACGAGCAGAGAGTCCT	
	Reverse: TTGCTGTAATGCTCGATGATG	210
SOX19A	Forward: GAGGATGGACAGCTACGG	
	Reverse: CTATAGGACATGGGGTTGTAG	179
NNR	Forward: GAGACATACCACAGGTGAAGC	
	Reverse: CCGCTCTGGTCTGTTGC	234

EGFP, enhanced green fluorescent protein; GRHL3, grainyhead-like transcription factor 3; SOX19A, SRY-box transcription factor 19a; NNR, nanor.

Assay for transposase-accessible chromatin with sequencing (ATAC-Seq). HeLa cells (Shanghai Tongpai Biotechnology Co., Ltd.) were seeded ($1x10^5$ cells/well) in 24-well plates and cultured in Dulbecco's Modified Eagle Medium (cat no. 10566016, Thermo Fisher Scientific, Inc.) with 10% fetal bovine serum (cat no. ZF181FBS-500, Zeta Life Co., Inc.) at 37˚C with 5% CO_2. The cells ($2x10^5$ cells/well) were transfected with C1-ORF2 vector (0.2 μg/μl) using Lipofectamine®2000 (Thermo Fisher Scientific, Inc.) at room temperature for 5 min, following the manufacturer's protocol. After 48 h, cells were grown in selective medium containing 1 mg/ml G418 (Beijing Biotopped Life Sciences, Inc.) for approximately 3 weeks. Then, the cells stably transfected with C1-ORF2 were obtained. LV (1.18 μg/μl) was added into stably transfected HeLa cells for 48 h. Same volume saline was added into stably transfected HeLa cells as a control. ATAC-seq was performed by Shanghai Jiayin Biotechnology Ltd. using a Novaseq 6000 Sequencing System (Illumina, Inc.) as previously described (30,31). Trimmomatic software (version 0.36, usadellab.org/cms/?page=trimmomatic) was used for quality control. Burrows Wheeler Aligner-maximal exact matches software (version 0.7.13-r1126, bio-bwa.sourceforge.net/) compared the clean data to the reference (CMV-EGFP-ORF2-PolyA) (32). MACS2 software (version 2.1.2, pypi.org/project/MACS2/) was used for analysis, and Q<0.05 was used as the screening threshold. DeepTools software (3.4.3, deeptools.readthedocs.io/en/develop/) was used to analyze signal distribution near to the CMV-EGFP-ORF2-PolyA reference.

DNase I digestion. C1-ORF2-histone-LV and C1-Alux14-histone-LV recombinants were obtained by the incubation reconstitution (see subsection: *In vitro* chromatin reconstitution). The recombinants were digested with 0.045 U/μl DNase I for 0 sec, 30 sec, 2 min or 4 min at room temperature. Next, the recombinants of C1-ORF2-histone-LV and C1-ORF2-histone-BSA were obtained using the dialysis recombination. Briefly, 100 μl of four different recombinant solutions were digested with DNase I (0.02, 0.04 or 0.08 U/μl) at room temperature for 1 min. Aliquots 10 μl termination solution (0.1 % SDS-10 mmol/l EDTA) was added and then precipitated with absolute ethyl alcohol. The precipitates were washed twice with 75% ethanol, dried, dissolved with 50 μl 2.5% SDS and 1/10 volume of xylene cyanol FF loading buffer. Each 10 μl sample was loaded into one lane and subject 1.5% agarose gel electrophoresis.

Statistical analysis. Each experiment was repeated at least three times. Data are presented as the mean ± standard deviations (SD). Statistical analysis was performed using SPSS software (version 17.0; IBM Corporation) and GraphPad Prism (version 6.0; Dotmatics). Group differences were assessed using one-way ANOVA with Tukey's post hoc test. P<0.05 was considered to indicate a statistically significant difference.

Results

L1-ORF2 enhances EGFP expression in EZEs. To determine whether human L1-ORF2 enhances EGFP expression in EZEs, C1-ORF2, C1-Alux14, C1-LacZ and pEGFP-C1 (C1) expression vectors were injected into 0 hpf ZEs and subsequently the EGFP fluorescence intensity was observed at 24 h post-injection. Brightest EGFP fluorescence was observed in the C1-ORF2 group (Fig. 1A and B). C1-ORF2 was injected into 0 hpf ZEs and the EGFP fluorescence intensity was observed at 6, 12, 24 and 48 h post-injection. EGFP fluorescence intensity induced by C1-ORF2 increased with time (Fig. 1C and D). However, when C1-ORF2 was injected into 0, 2 and 4 hpf ZEs, EGFP fluorescence intensity of 0 hpf was higher than of 2 hpf and 4 hpf groups, which indicated that EGFP expression is related to embryo development stage (Fig. 1E and F). Taken together, these results suggested that the developmental stage affected expression of EGFP induced by C1-ORF2 in EZEs. To determine whether ORF2 activates EGFP via transcriptional changes, RT-qPCR was used to quantify EGFP mRNA. C1-ORF2 significantly increased expression of EGFP mRNA compared with C1-Alux14 or C1-LacZ vectors (Fig. 1G). These results suggested that ORF2 could activate *EGFP* gene expression at the transcriptional level.

To exclude any enhancer role of poly(A) on *EGFP* activation, poly(A) was removed from the C1 plasmid, generating C1-delPolyA. The C1, C1-ORF2, C1-delPolyA, C1-delPolyA-ORF2 and C1-delPolyA-ZORF2 vectors were injected into EZEs and the lowest EGFP fluorescence intensity was observed in the C1-delPolyA group, whereas the EGFP fluorescence intensity induced by C1-delPolyA-ORF2 and C1-delPolyA-ZORF2 were significantly higher compared with

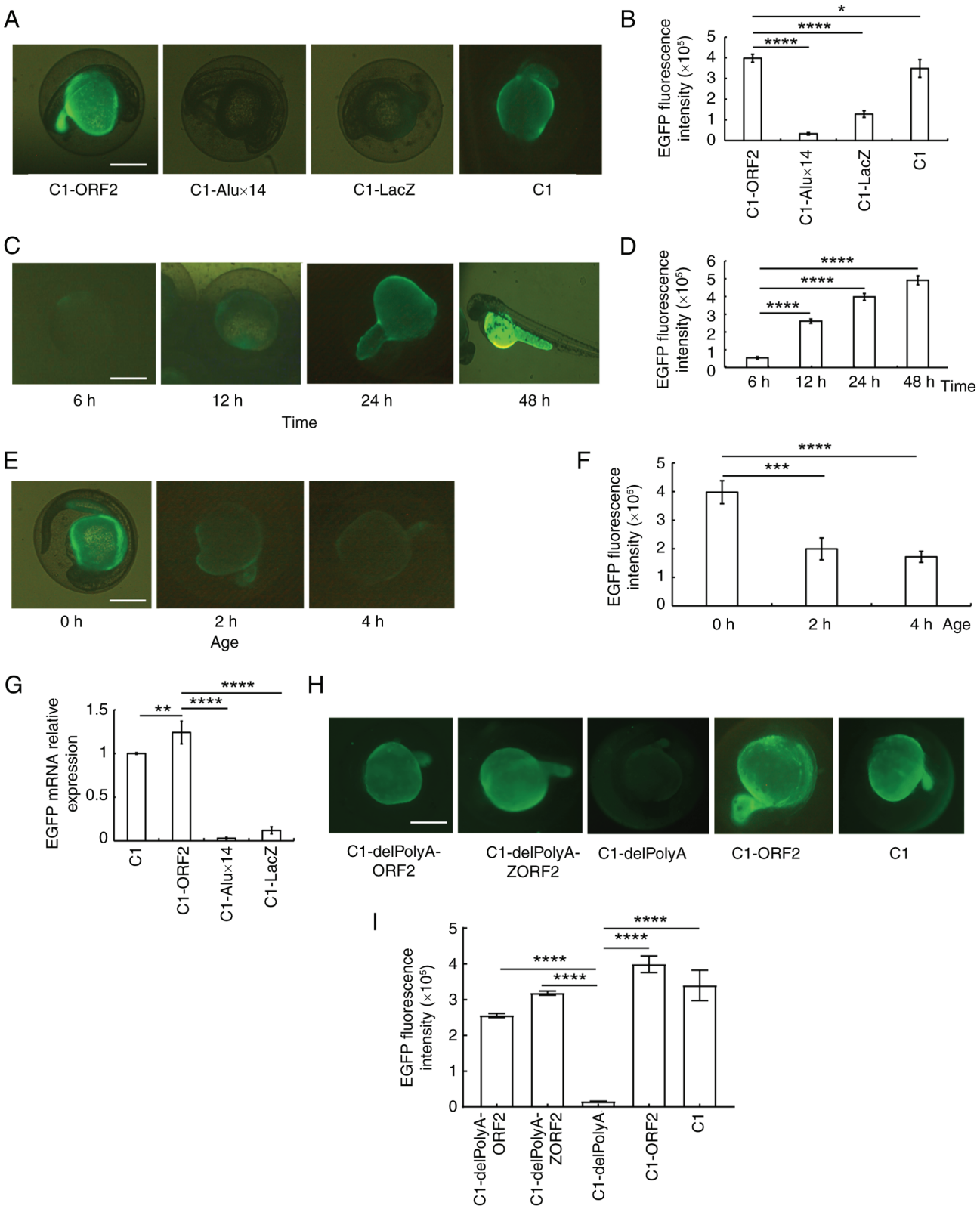

Figure 1. ORF2 activates EGFP expression in 0 h zebrafish embryos. (A) EGFP fluorescence (B) intensity following injection of the C1-ORF2, C1-Alux14, C1-LacZ or C1 (pEGFP-C1) vectors. (C) EGFP fluorescence (D) intensity after C1-ORF2 injection. (E) EGFP fluorescence (F) intensity induced by C1-ORF2 injection into embryos at different developmental stages, observed after 24 h. (G) ORF2 activates EGFP expression at the transcriptional level. (H) EGFP fluorescence (I) intensity at 24 h after injection of C1-delPolyA-ORF2, C1-delPolyA-ZORF2, C1-delPolyA, C1-ORF2 and C1. Scale bar, 200 μm. *P<0.05, **P<0.01, ***P<0.001, ****P<0.0001. EGFP, enhanced green fluorescent protein; ORF2, open reading frame 2.

that induced by C1-delPolyA (Fig. 1H and I). These results further demonstrated that ORF2 activated EGFP gene expression in EZEs.

Histone inhibits EGFP expression induced by ORF2, which is negated by ZEL. To observe the effects of histone on ORF2-induced EGFP expression in EZEs, C1-ORF2 was

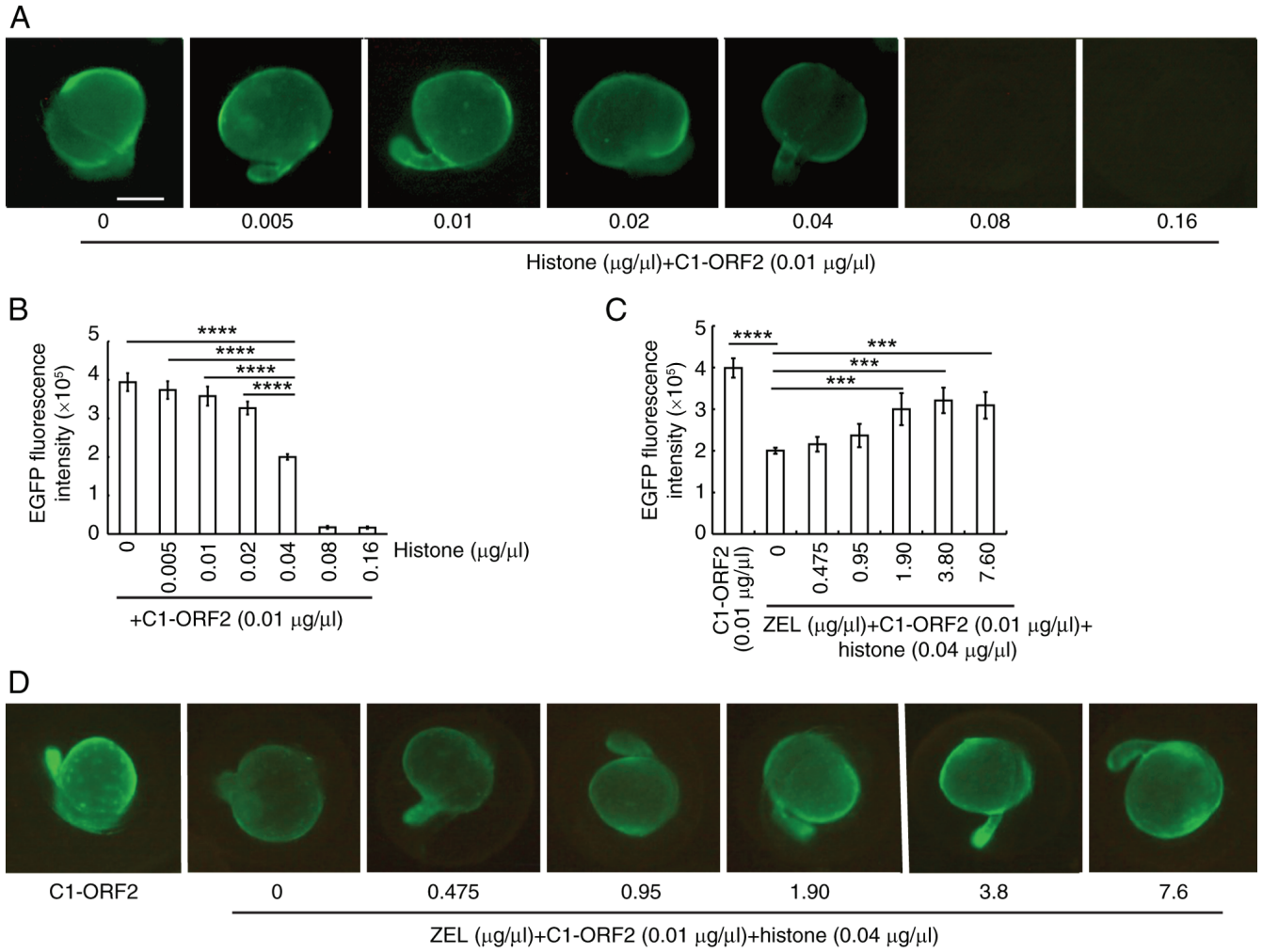

Figure 2. ZEL attenuates histone-dependent suppression of C1-ORF2 EGFP fluorescence. (A) EGFP fluorescence (B) intensity following incubation with histone. (C) EGFP fluorescence intensity (D) induced by C1-ORF2 following incubation with 0.04 μg/μl histone and ZEL. Scale bar, 200 μm. ***P<0.001, ****P<0.0001. ZEL, zebrafish embryo lysate; EGFP, enhanced green fluorescent protein; ORF2, open reading frame 2; OD, optical density.

incubated with histone and injected into 0 hpf ZEs. EGFP expression was then observed at 24 h post-injection. EGFP fluorescence decreased as histone concentration increased (Fig. 2A). Upon incubation with 0.04 μg/μl histone, the intensity of EGFP induced by ORF2 decreased by almost 50% compared with 0 μg/μl histone (Fig. 2B).

Based on relative levels of histones and transcription factors, which both regulate the onset of transcription in the EZEs (33), it was hypothesized that ZEL contains certain components that eliminate the inhibitory effect of histones on C1-ORF2. As the concentration of ZEL increased, the inhibitory effect induced by histones decreased (Fig. 2D); 3.8 μg/μl ZEL could eliminate 80.49% of the histone-mediated inhibition of EGFP expression (Fig. 2C). These findings indicated that ZEL attenuates the suppression of ORF2-dependent EGFP expression by histone.

LV ameliorates histone-induced inhibition and enhances expression of EZE genes. It was hypothesized that DNA-binding proteins of the ZEL could activate EGFP fluorescence via interaction with C1-ORF2 in 0 hpf ZEs. Salmon sperm DNA was incubated with ZEL and the key proteins were divided according to their molecular mass (~115, ~100 and ~25 kDa; Fig. 3A and B).

LV was purified from ZEL. The purified LV was analyzed using Easy-nLC1200 high-performance liquid chromatography (Table SI). The different concentrations of LV (0, 0.625, 1.25, 2.5, 5.0 and 10 μg/μl) were incubated with histone and C1-ORF2. LV could attenuate the inhibitory effect of histone on C1-ORF2-induced EGFP expression (Fig. 3C and D); by contrast, BSA failed to alleviate the inhibitory effect of histone on EGFP expression at any concentration (Fig. 3E).

MZP, which does not contain LV, was used as an appropriate control for demonstrating the specificity of LV. MZP was found not to attenuate histone-induced inhibition on EGFP expression (Fig. 4A and B). Globin is an abundant protein in MZP, with a molecular weight of ~13 kDa (34,35). SDS-PAGE showed that globin was one of the abundant proteins in MZP (Fig. 4C). Different concentrations of globin did not weaken histone-induced inhibition (Fig. 4D and E).

In a previous study, the concentration of LV was higher in good- compared with poor-quality eggs (36). To explore the role of LV in EGFP gene activation, C1-delPolyA, C1-delPolyA-ORF2 and C1-delPolyA-ZORF2 were injected into 0 hpf ZEs with poor or good quality, and EGFP fluorescence was observed at 24 h post-injection. ORF2 and ZORF2

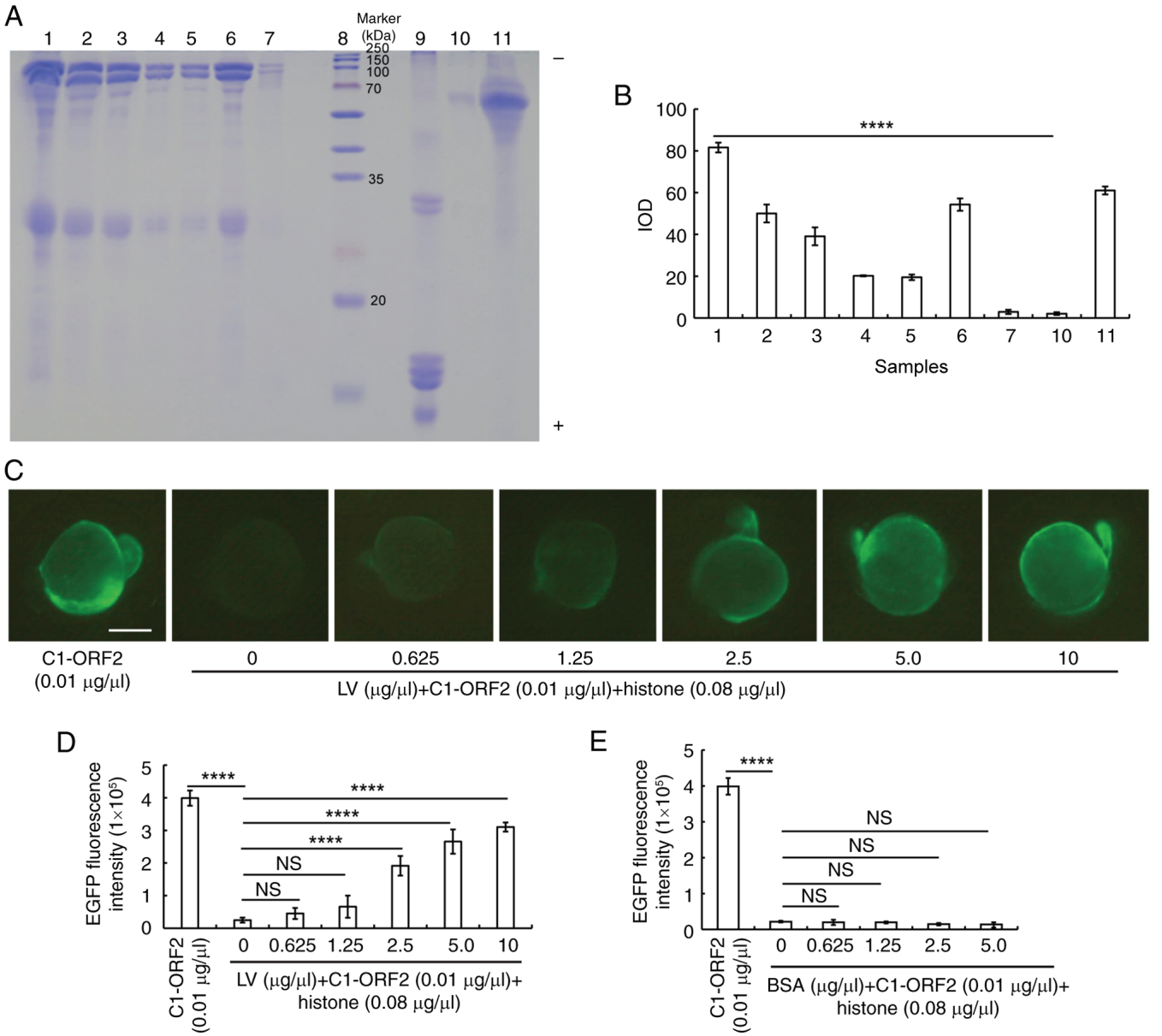

Figure 3. LV alleviates histone-induced inhibition. (A) SDS-PAGE of ZEL incubated with salmon-sperm DNA. Lanes 1-4, First to fourth precipitate of salmon-sperm DNA and ZEL, the supernatant of the fourth precipitate (lane 5), ZEL (lane 6), diluent (lane 7), Marker (lane 8), histone (lane 9), precipitate of salmon-sperm DNA and FCS (lane 10) and FCS (lane 11). (B) IOD. (C) EGFP fluorescence (D) intensity induced by C1-ORF2 incubated with histone and LV (scale bar, 200 μm). (E) Embryos showing EGFP fluorescence induced by C1-ORF2 incubated with histone and BSA. ****P<0.0001. NS, not significant; LV, lipovitellin; ZEL, zebrafish embryo lysate; EGFP, enhanced green fluorescent protein; ORF2, open reading frame 2; IOD, integrated optical density.

could induce strong EGFP fluorescence in good- but not in poor-quality embryos (Fig. 5A and B).

An *in vitro* transcription assay was employed to explore whether LV serves a role in gene expression regulation. Histone inhibited EGFP transcription, whereas LV attenuated this inhibitory effect (Fig. 5C). LV increased the mRNA levels of the GRHL3, SOX19A and NNR (Fig. 5D).

To verify whether results were reflective of the role of LV in terms of regulating transcription of ZEs, LV was injected into the abdominal cavity of adult male zebrafish. RT-qPCR was then used to detect the expression levels of the GRHL3, SOX19A and NNR genes. LV could increase transcription of the GRHL3, SOX19A and NNR genes (Fig. 5E). Furthermore, RNA-seq method was used to detect the influence of LV on the gene expression profile of liver tissue. LV increased the transcription of SOX19A by 4.89-fold; RT-qPCR shows that LV increased the transcription level of SOX19A by 2.73-fold (Fig. 5E). However, GRHL3 and NNR genes were not detected by RNA-seq. Sensitivity of RNA-seq is lower than that of RT-qPCR (35). GO enrichment analyses showed that the upregulated genes induced by LV injection were significantly enriched in 'cell development' (Fig. 5F). These results demonstrated that LV increased the expression of genes associated with early embryo development.

LV binds ORF2 to loosen the structure of chromatin, subsequently regulating gene expression. As LV is primarily found in the yolk sac of embryo, it was important to ensure that LV could move into cell nucleus. FITC-LV was injected into the animal pole or yolk sac of ZEs at 0 or 3 hpf and

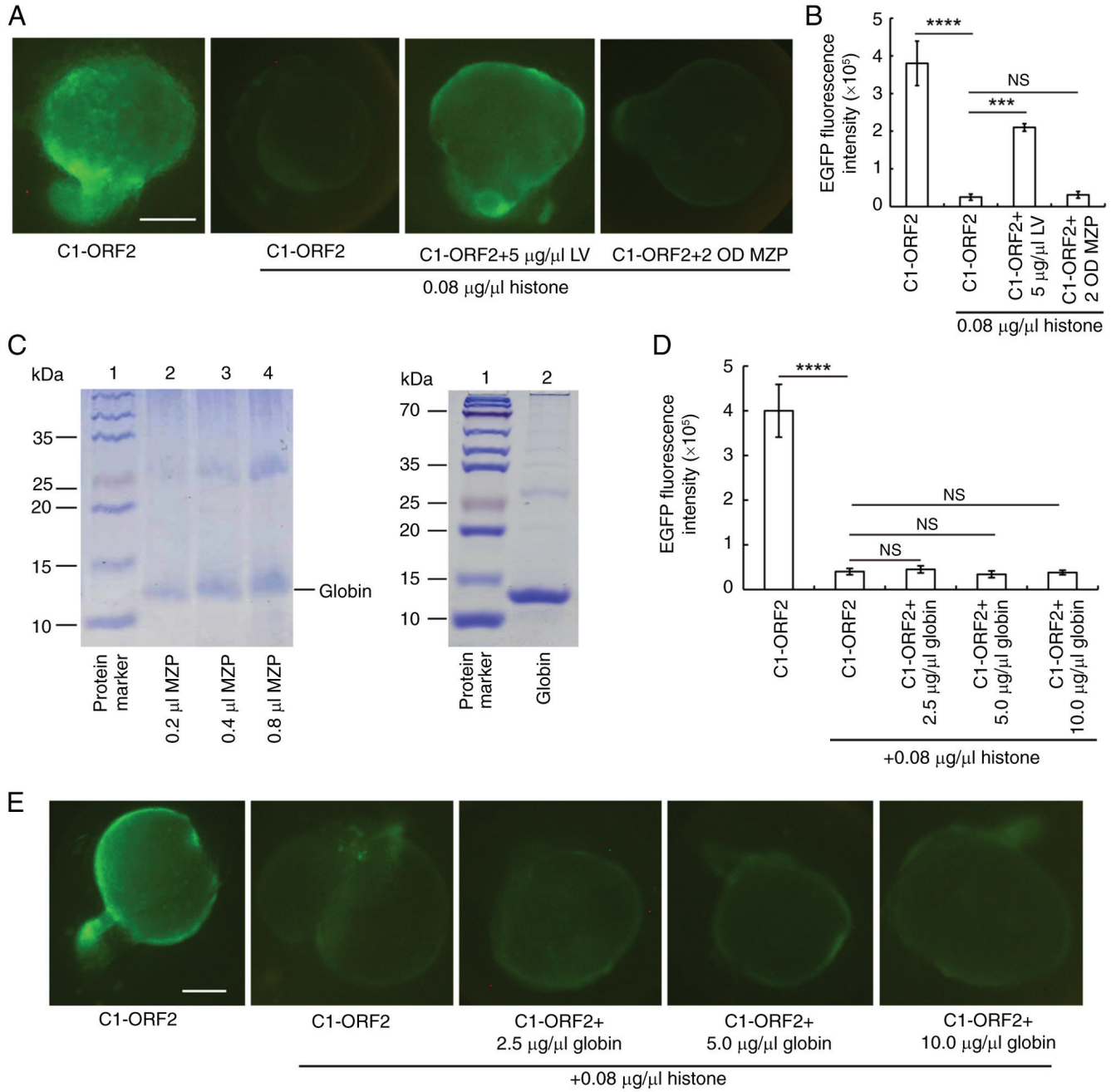

Figure 4. MZP and globin do not alleviate histone-induced inhibition. (A) EGFP fluorescence (B) intensity induced by C1-ORF2 incubated with histone and 5 μg/μl LV or 2 OD MZP. (C) Globin was purified from MZP. SDS-PAGE of MZP, showing that globin was the primary protein in MZP. (D) EGFP fluorescence induced by (E) C1-ORF2 incubated with histone and globin. Scale bar, 200 μm. ***P<0.001, ****P<0.0001. MZP, male zebrafish plasma; NS, not significant; LV, lipovitellin; EGFP, enhanced green fluorescent protein; ORF2, open reading frame 2; OD, optical density.

fluorescence was observed after 72 h. When FITC-LV was injected into the animal pole, green fluorescence was found in both zebrafish and cells, including the nucleus. This indicated that FITC-LV could cross the zebrafish cell and nuclear membrane (Fig. 6A and C). When FITC-LV was injected into the yolk sac of zebrafish embryo at 0 hpf, both zebrafish and cells (including nuclei) showed green fluorescence (Fig. 6B). However, when FITC-LV was injected into yolk sac of 3 hpf embryos, the fluorescence was only found in yolk sac (Fig. 6D). These findings indicated that FITC-LV was unable to penetrate the syncytial layer at 3 hpf of embryonic development.LV was passed through the cell and nuclear membrane and might therefore have an important role in early embryos.

Since LV serves an important role in gene regulation, the present study explored which DNA fragment best binds LV. ChIP analysis of the embryo tissue revealed LV bound ORF2 more readily than it did Alux14 (Fig. 7A). In addition, ORF2, Alux14 and C1 fragments were incubated with LV. EMSAs showed that the binding ability of ORF2 and LV was greater compared with that of LV with C1 or Alux14 (Fig. 7B and C).

LV could ameliorate the inhibitory effect on C1-ORF2 mediated by histone, To determine the underlying mechanism, histone, C1/ORF2 fragments and LV were mixed. Histone was

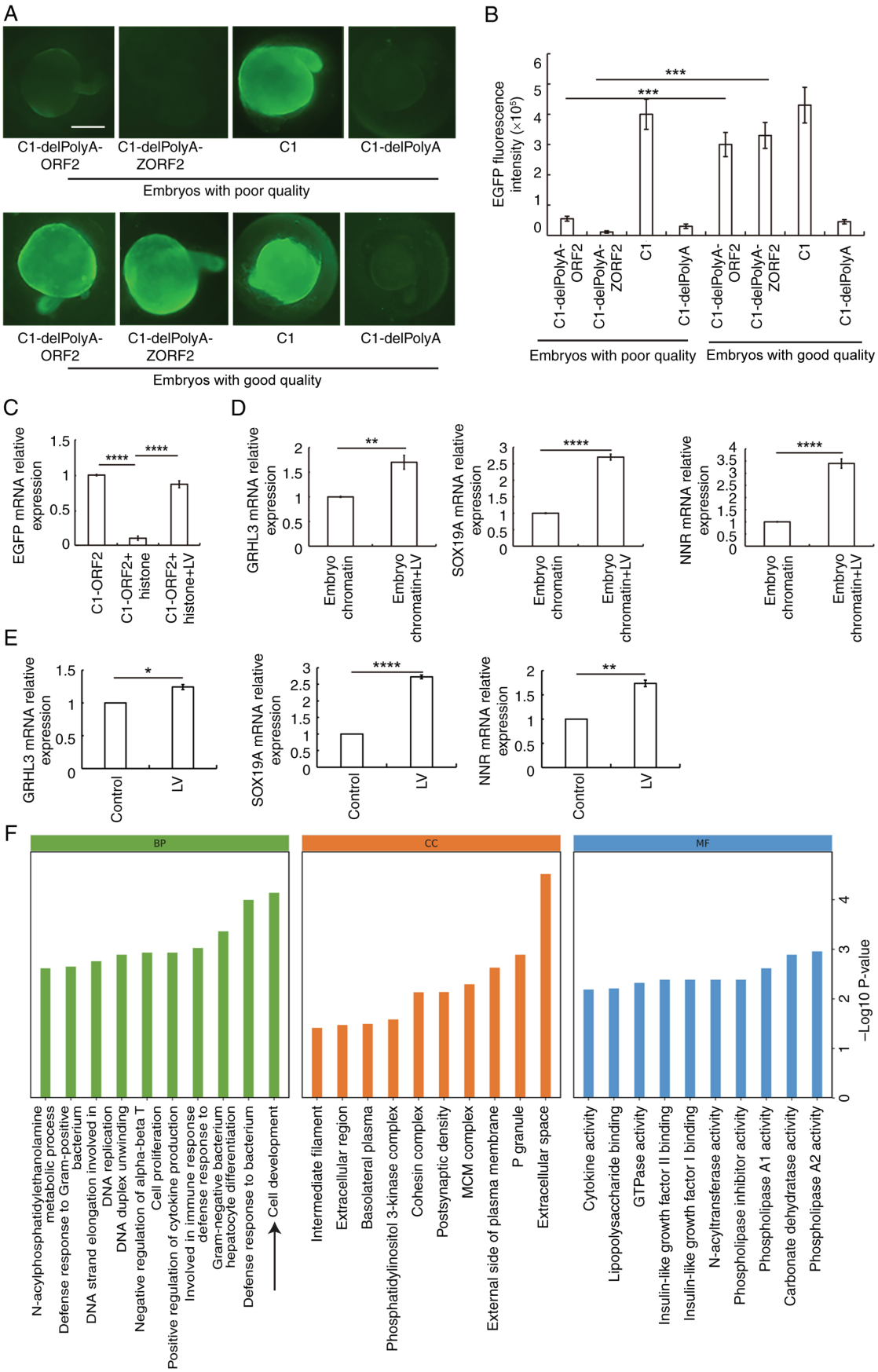

Figure 5. LV activates EGFP gene expression in good-quality 0 h ZEs and promotes expression both of EGFP reporter gene and genes of EZEs. (A) Embryos injected with C1-delPolyA-ORF2, C1-delPolyA-ZORF2, C1 and C1-delPolyA expression vectors. The scale bar represents 200 μm. (B) EGFP fluorescence intensity. (C) LV attenuates the inhibitory effect of histone on EGFP mRNA. LV promotes expression of GRHL3, SOX19A and NNR genes in (D) EZEs and (E) adult male zebrafish liver. *P<0.01, **P<0.01, ***P<0.001, ****P<0.0001. (F) GO gene function classification. GO, Gene Ontology; GRHL3, grainyhead-like transcription factor 3; SOX19A, SRY-box transcription factor 19a; NNR, nanor. BP, biological process; CC, cell component; MF, molecular function; LV, lipovitellin; EGFP, enhanced green fluorescent protein; ORF2, open reading frame 2.

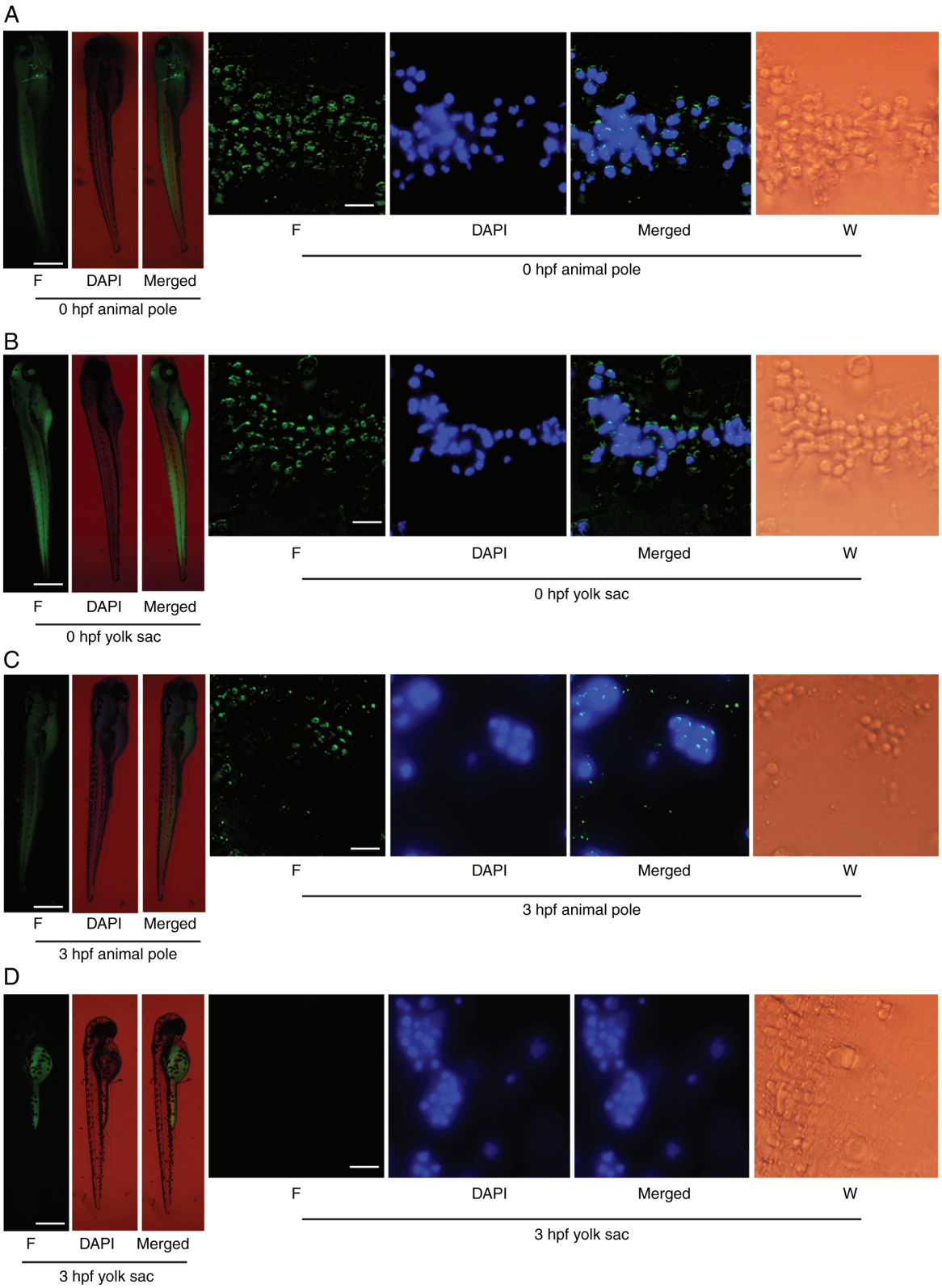

Figure 6. FITC-LV enters zebrafish embryo cells and nuclei. Representative images of the zebrafish larvae and cells when FITC-LV was microinjected into 0 hpf (A) animal pole, 0 hpf yolk sac (B), 3 hpf animal pole (C) and 3 hpf yolk sac (D), observed after 72 h. The scale bar on the fish image represents 500 μm. The scale bar on the cell image is 20 μm. LV, lipovitellin; F, fluorescence; W, white light; hpf, h post-fertilization.

incubated with LV and C1/ORF2 fragments. EMSA showed that C1/ORF2 fragments underwent complete hysteresis at 0 μg/μl LV (Fig. 8A, lane 2). With increasing LV concentrations (0.0125 and 0.0625 μg/μl), both C1 and ORF2 underwent partial gel shifts (Fig. 8A; lanes 3 and 4); but when LV concentration was high (0.03125 μg/μl), the C1 and ORF2 fragments underwent complete shifts (Fig. 8A, lane 5). When C1/ORF2 fragments were incubated with histone first and subsequently

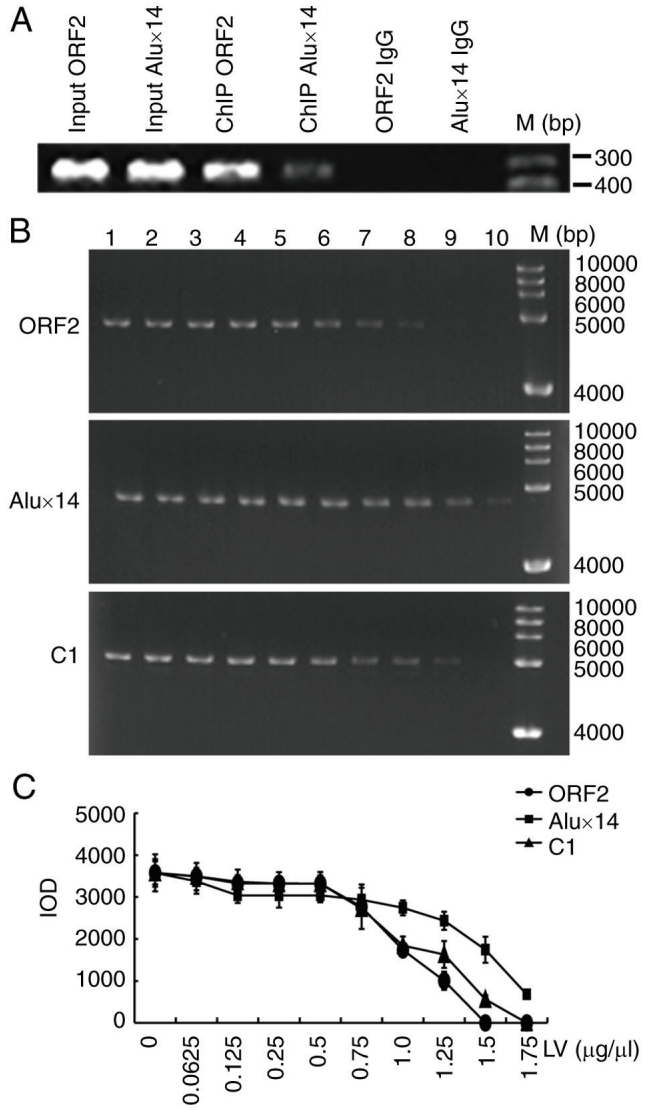

Figure 7. LV binds ORF2 more readily than with Alux14. (A) ChIP analysis of LV binding to ORF2 or Alux14. Rabbit-IgG immunoprecipitate was used as the negative control. (B) Purified ORF2, Alux14 or C1 fragments were incubated with LV in EMSA. 1-10 lanes: 0, 0.0625, 0.125, 0.25, 0.5, 0.75, 1.0, 1.25, 1.5 and 1.75 μg/μl LV.M, Marker. (C) IOD value. IOD, integrated optical density; LV, lipovitellin; ORF2, open reading frame 2; ChIP, chromatin immunoprecipitation assay; EGFP, enhanced green fluorescent protein.

with LV, all concentrations of LV caused complete gel retardation of the C1 and ORF2 fragments (Fig. 8A). Similarly, when C1/ORF2 fragments were incubated with LV first and with histone, all concentrations of LV caused complete gel retardation of the C1 and ORF2 fragments (Fig. 8A). Fig. 8B shows the sum of the IOD values of the C1 and ORF2 fragments in each lane. Subsequently, effects of histone concentration on gel retardation when histone was incubated with LV prior to addition of C1/ORF2 were examined. LV induced the partial shift of C1/ORF2 with 0.015 μg/μl, 0.02 and 0.025, but not 0.03 μg/μl histone (Fig. 8C and D).

Transcription factors act on specific regions of chromatin to improve chromatin accessibility, manifested as an increased sensitivity to DNase I digestion (37). The present study investigated whether LV was able to promote the sensitivity of C1-ORF2 to DNase I digestion. C1-ORF2 DNA was more easily digested compared with C1-Alux14 (Fig. 9A and B). LV or BSA was incubated with C1-ORF2 and histone by salt-dialysis reconstitution and digested with different concentrations of DNase I. The brightness of the C1-ORF2 fragments incubated with LV was significantly lower compared with BSA when digested using the same concentration of DNase I (Fig. 9C and D). Taken together, these results suggested that LV promoted sensitivity of C1-ORF2 to DNase I digestion, which indicated that LV increased the chromatin accessibility of C1-ORF2 recombinant.

To verify that LV was able to improve chromatin accessibility of the cytomegalovirus (CMV) region (enhancer and promoter) of the EGFP gene in the C1-ORF2 plasmid, HeLa cells were stably transfected with C1-ORF2 plasmid and treated with LV. ATAC-seq was performed to measure the degree of chromatin opening in the CMV region of the EGFP gene in stably transfected plasmids. There were more CMV-area ATAC-seq signals in the LV compared with the control group (Fig. 9E and F). Taken together, the results of ATAC-seq confirmed that LV enhanced the CMV chromatin accessibility of C1-ORF2, consistent with the DNase I digestion experiments.

Discussion

L1 is dynamically expressed in early embryos, although its expression decreases with embryonic development (10,38,39). Here, C1-ORF2 could induce the high expression of EGFP gene in 0 hpf ZEs, whereas C1-Alux14 or C1-LacZ could not. However, when C1-ORF2 was transfected into HeLa cells, the EGFP gene was almost non-expressed (16,40). To exclude the enhancer role of poly(A) on EGFP gene expression, poly(A) was removed from the C1 plasmid to generate C1-delPolyA expression vector and both human ORF2 and zebrafish ORF2 (ZORF2) were inserted into C1-delPolyA. In the absence of poly(A), both ORF2 and ZORF2 induce EGFP expression in 0 hpf ZEs.

The relative levels of histone and transcription factors regulate onset of transcription in embryos (33). Methylcytosine-modifying 10-11-translocation 1 activates L1 by attenuating histone repression (41,42). In the present study, histone decreased EGFP expression and ZEL eliminated histone inhibition in 0 hpf ZEs. Therefore, it was hypothesized that a component of the ZEL could reduce histone inhibition.

EZEs contain various DNA-binding proteins that fulfill important roles in the zygotic genome activation (43). It has been reported that purified zebrafish LV is a phospholipoglycoprotein with molecular mass of ~445 kDa, which can be resolved into polypeptides corresponding to ~117, ~102 and ~23.8 kDa by SDS-PAGE (44). Therefore, the DNA-binding proteins in the ZEL were identified by SDS-PAGE following precipitation of DNA. LV was the most abundant protein in the precipitate. As a predominant DNA-binding protein in embryos, LV is involved in lipid and metal storage and is utilized gradually during embryonic development (13,45); several proteins have been shown to regulate L1 expression (46); therefore, LV may serve an important role in regulating L1 expression. Furthermore, purified LV was shown to attenuate histone-induced inhibition similarly to ZEL. In addition, it was shown that neither ORF2 nor ZORF2 induced EGFP expression in poor-quality embryos, which were similar

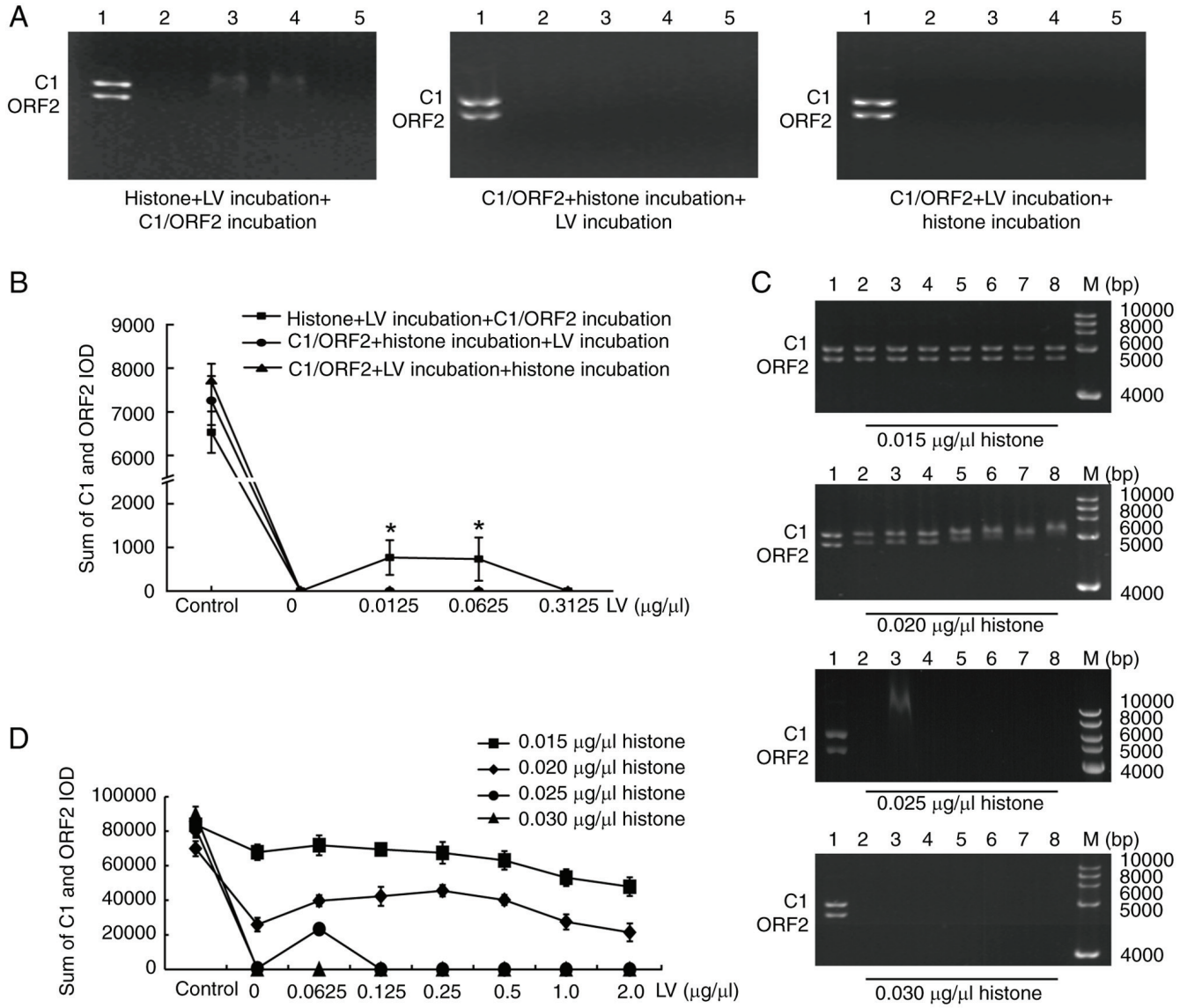

Figure 8. LV interferes with histone binding to C1 and ORF2 sequence. (A) EMSA following incubation of LV with histone and C1-ORF2. Left, histone was incubated with LV, and incubated with C1/ORF2 fragments; middle, histone was incubated with C1/ORF2 fragments, and with LV; right, LV was incubated with C1/ORF2 fragments, then with histone. 1, control group, 2-5 lanes: 0, 0.0125, 0.0625 and 0.3125 μg/μl LV. (B) IOD values of the C1 and ORF2 fragments in each lane. (C) Effect and (D) IOD of histone concentrations on gel retardation when histone was first incubated with LV, and with C1/ORF2. 1-8 lanes: 0, 0.0625, 0.125, 0.25, 0.5, 1.0 and 2.0 μg/μl LV, lipovitellin; ORF2, open reading frame 2; IOD, integrated optical density; M, Marker.

to embryos featuring LV knockout (36). Therefore, LV might affect ORF2 expression.

Furthermore, LV increased the EGFP mRNA levels when incubated with the C1-ORF2. The GRHL3, SOX19A and NNR genes have been shown to be EZE expression genes (47,48). Both *in vitro* transcription system and *in vivo* LV injection experiments showed that LV increased the mRNA expression levels of the EZE genes GRHL3, SOX19A and NNR. Therefore, LV may be the regulating factor of ORF2 in early embryos.

When FITC-LV injected into yolk sac of zebrafish, FITC-LV could penetrate into the cytoplasm and nucleus in 0 but not 3 hpf embryos. In 3 hpf embryos, the embryo genome is transcriptionally activated and cells were able to synthesize the required proteins by themselves, so LV may regulate gene expression only in the early embryos (49).

Multiple DNA-binding proteins affect gene transcription, and several proteins regulate L1 expression (46). ChIP analysis and EMSAs showed that the affinity between ORF2 DNA and LV was higher compared with between Alux14 and LV. These results suggested that LV may be an activator of ORF2; however, the underlying mechanism governing how LV regulates ORF2 transcription and acts as a trans-acting factor has yet to be elucidated.

Competition between histone and transcription factor binding regulates the onset of transcription in ZEs (33). The present study identified a decrease in C1/ORF2 gel retardation when LV was incubated with histone before addition of ORF2. Histone is a universal DNA-binding protein that forms octamers to package DNAs. Histone has a higher binding stability compared with other DNA-binding proteins; therefore, transcription factors activate gene expression only prior to histone binding to DNA (50). Theoretically, binding of proteins to histone could also delay histone from packaging the DNA. In the present study, only the pre-incubation of LV with histone could

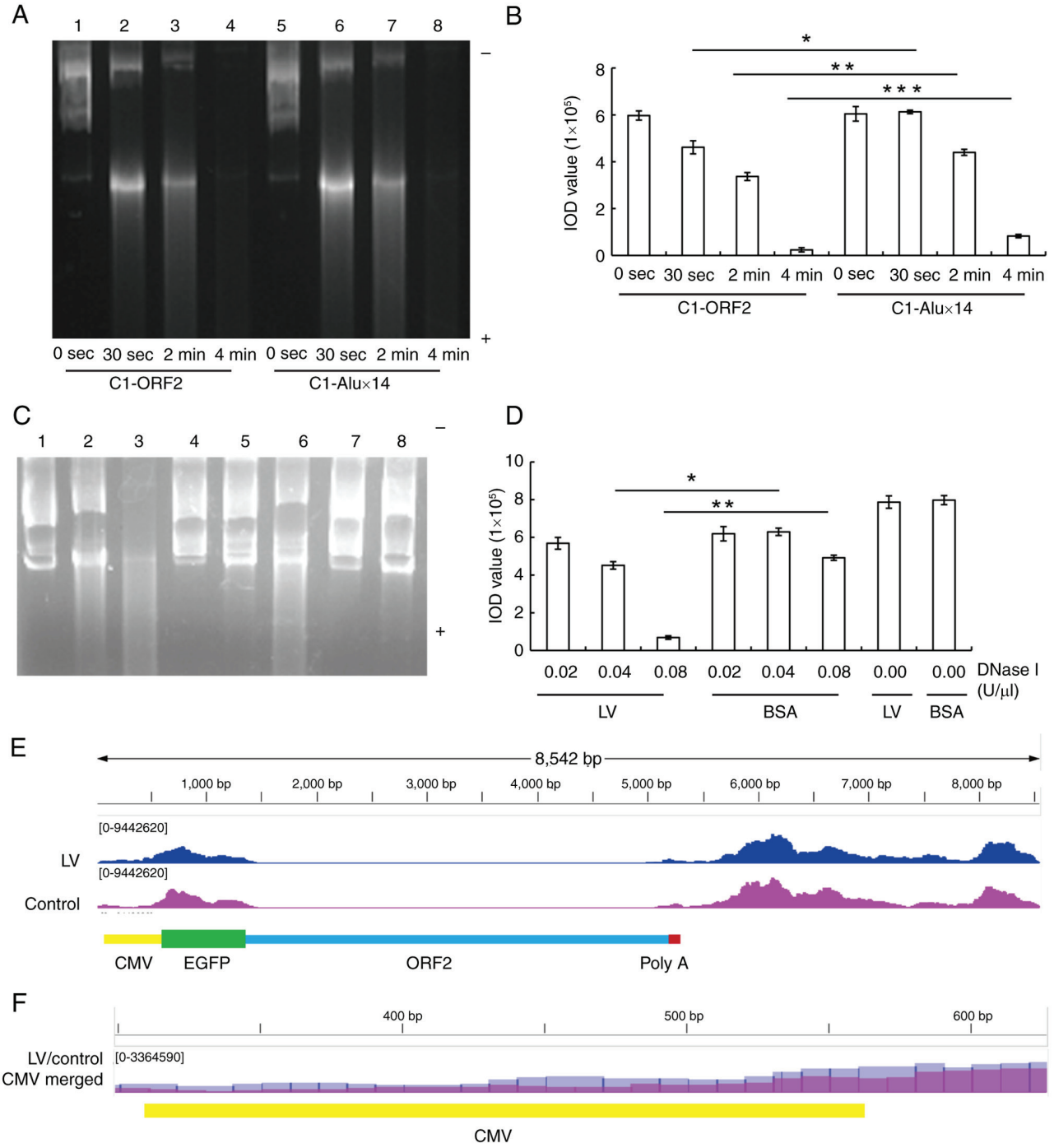

Figure 9. LV increases DNase I digestion-sensitivity of C1-ORF2. (A) Representative DNase I digestion of C1-ORF2 + histone + LV (C1-ORF2) or C1-Alux14 + histone + LV (C1-Alux14) recombinants. (B) IOD values of each lane. (C) Representative image showing DNase I digestion according to the salt-dialysis reconstitution method. C1-ORF2 (0.06 μg), histone (0.18 μg) and 3 μg LV (or BSA) were recombined using the salt-dialysis reconstitution method. The recombinants were digested for 1 min with 0.02, 0.04 or 0.08 U/μl DNase I. 1-3 lanes: 0.02, 0.04 and 0.08 μg/μl LV; 4-6 lanes: 0.02, 0.04 and 0.08 μg/μl BSA; 7 lane: 0.00 μg/μl LV; 8 lane: 0.00 μg/μl BSA. (D) IOD values of each lane. (E) C1-ORF2 ATAC-seq signals. CMV area (CMV enhancer and promoter) ATAC-seq signals in the LV treatment group were stronger than those in control group. (F) Amplified CMV ATAC-seq signals in the LV (blue) and control (purple) group. CMV ATAC-seq signals in the LV group were more numerous than those in the control group. *P<0.01, **P<0.01, ***P<0.001. LV, lipovitellin; ORF2, open reading frame 2; IOD, integrated optical density, ATAC-seq, assay for transposase-accessible chromatin with sequencing; CMV, cytomegalovirus enhancer and promoter.

reduce C1/ORF2 gel retardation that was caused by histone, indicating that LV had the capability of binding to histone. The histone in the ZEL is bound to the histone chaperone molecule, rather than being isolated (51), suggesting that LV is also a type of chaperone molecule. LV therefore exerts an important role in balancing the binding of histone to DNA.

Chromatin accessibility is directly associated with transcription in eukaryotes (52). Accessible regions associated with regulatory proteins are highly sensitive to DNase I digestion (37). The present study demonstrated that LV attenuated inhibition of histone-induced EGFP expression in the C1-ORF2 vector. Chromatin was reconstituted using

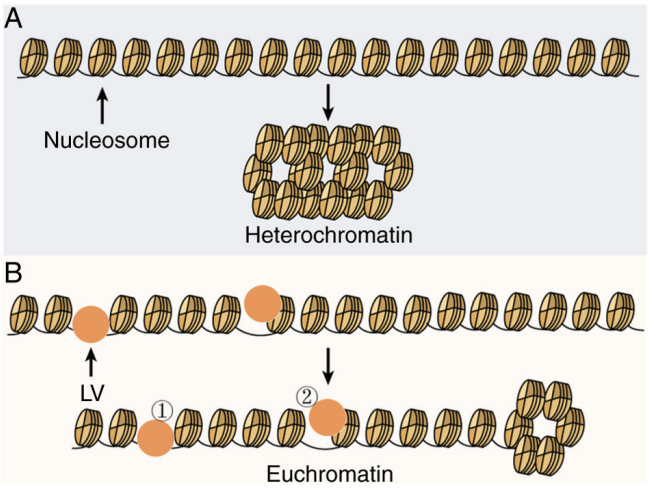

Figure 10. Alternative molecular mechanisms to account for how LV may increase expression of ORF2-induced EGFP gene in zebrafish embryos. (A) Putative mechanism of decreased L1-ORF2 accessibility involves packaging of histone and L1-ORF2 into heterochromatin in the absence of LV. (B) Putative mechanism of increased L1-ORF2 accessibility. In the presence of LV, histones and L1-ORF2 are packaged as euchromatin. LV binding to 1, DNA and 2, histone. LV, lipovitellin; ORF2, open reading frame 2; EGFP, enhanced green fluorescent protein.

LV, histones and C1-ORF2 (or C1-Alux14) and the DNase I digestion showed that LV, but not BSA, promoted DNase I digestion sensitivity of recombinant C1-ORF2. ATAC-seq is a novel method to detect chromatin accessibility (53). ATAC-seq was used to verify whether LV enhanced chromatin accessibility; LV induced more ATAC-seq signals in the CMV area when LV was added to C1-ORF2 stably transfected HeLa cells.

The present study demonstrated that LV attenuates the inhibitory effect of histone on ORF2-induced EGFP reporter gene expression, upregulated expression of EZE genes both *in vivo* and *in vitro*, bound ORF2 DNA and histones and increased accessibility of C1-ORF2 DNA. Binding of DNA with histones forms nucleosomes, which are packaged into heterochromatin, inhibiting gene expression (54,55). LV interferes with nucleosome packaging by binding ORF2 DNA and histones, which prevents the formation of heterochromatin, which promotes DNA transcription. The present study has suggested that LV interfered with the binding of histones to ORF2 DNA through binding with both ORF2 and histones. Dissociation of histones from the ORF2 DNA results in a loosening of ORF2 DNA (56). When histone binds to LV, a complex of histone and LV is formed (histone-LV), which decreases and interferes with binding between histone and DNA (57).

Fig. 10 shows potential molecular mechanisms that may explain how LV increases expression of the ORF2-induced EGFP gene and EZE-associated genes in ZEs. The packaging of histone and L1-ORF2 into heterochromatin in the absence of LV caused the decreased L1-ORF2 accessibility, however the presence of LV increased L1-ORF2 accessibility due to LV interfering with the tight packaging of ORF2 DNA by histones. To the best of our knowledge, the present study is the first to demonstrate that LV is the main DNA-binding protein in ZEL, acting as a trans-acting factor. The binding of LV to DNAs had sequence specificity and LV had greater affinity for the ORF2 fragment. LV bound histone to interfere with binding between histone and DNA and promoted ORF2-induced high expression of EGFP gene by increasing the accessibility of ORF2-containing DNA constructs and expression of development-associated genes.

The present study found that LV is a regulating factor of ORF2; however, the present study had limitations. During early embryonic development, gene expression regulation involves proteins, protein and DNA modifications and RNAs (58); therefore, further studies should consider the potential synergistic effect of LV with other gene expression factors. LV affected the expression of the EGFP gene induced by both the ZORF2 and ORF2. There is no LV component in human embryos, although human ORF2 is also highly expressed in early human embryos, suggesting that equivalent components of LV are also present in human early embryos (59). These should be identified in future.

Acknowledgements

Not applicable.

Funding

The present study was supported by National Natural Science Foundation of China (grant no. 81771499), Natural Science Foundation of Hebei Province, China (grant nos. H2018206099 and H2021206460) and Science and Technology Research Project of Colleges and Universities in Hebei Province (grant no. ZC2016057).

Availability of data and materials

The data generated in the present study may be found in the Science Data Bank under accession number (31253.11. sciencedb.12153 and 31253.11. sciencedb.13038) or at the following URL: doi.org/10.57760/sciencedb.12153 and doi.org/10.57760/sciencedb.13038).

Authors' contributions

NJ, CGW and WXW conceived and designed the study and performed experiments. XDW, YZ, LA, ZXS performed experiments and analyzed and interpretation of data. GZ, XF and YW analyzed and interpreted the data and reviewed the manuscript. ZJL and XW designed experiments, wrote the manuscript and analysis data. ZJL and XW confirm the authenticity of all the raw data. All authors have read and approved the final manuscript.

Ethics approval and consent to participate

Experiments were approved by the Committee on Ethics of Animal Experiments of Hebei Medical University (approval no. IACUC-Hebmu-2021009).

Patient consent for publication

Not applicable.

Competing interests

The authors declare that they have no competing interests.

References

1. Percharde M, Lin CJ, Yin Y, Guan J, Peixoto GA, Bulut-Karslioglu A, Biechele S, Huang B, Shen X and Ramalho-Santos M: A LINE1-nucleolin partnership regulates early development and ESC identity. Cell 174: 391-405.e19, 2018.
2. Milioto V, Perelman PL, Paglia L, Biltueva L, Roelke M and Dumas F: Mapping retrotransposon LINE-1 sequences into two cebidae species and homo sapiens genomes and a short review on primates. Genes (Basel) 13: 1742, 2022.
3. Otsu M and Kawai G: Distinct RNA recognition mechanisms in closely related LINEs from zebrafish. Nucleosides Nucleotides Nucleic Acids 38: 294-304, 2019.
4. Wang F, Chamani IJ, Luo D, Chan K, Navarro PA and Keefe DL: Inhibition of LINE-1 retrotransposition represses telomere reprogramming during mouse 2-cell embryo development. J Assist Reprod Genet 38: 3145-3153, 2021.
5. Tiwari B, Jones AE, Caillet CJ, Das S, Royer SK and Abrams JM: p53 directly represses human LINE1 transposons. Genes Dev 34: 1439-1451, 2020.
6. Kajikawa M, Sugano T, Sakurai R and Okada N: Low dependency of retrotransposition on the ORF1 protein of the zebrafish LINE, ZfL2-1. Gene 499: 41-47, 2012.
7. Peterson CL and Hansen JC: Chicken erythrocyte histone octamer preparation. CSH Protoc 2008: pdb.prot5112, 2008.
8. Wehbi SS and Zu Dohna H: A comparative analysis of L1 retrotransposition activities in human genomes suggests an ongoing increase in L1 number despite an evolutionary trend towards lower activity. Mob DNA 12: 26, 2021.
9. Garcia-Cañadas M, Sanchez-Luque FJ, Sanchez L, Rojas J and Garcia Perez JL: LINE-1 retrotransposition assays in embryonic stem cells. Methods Mol Biol 2607: 257-309, 2023.
10. Chang NC, Rovira Q, Wells J, Feschotte C and Vaquerizas JM: Zebrafish transposable elements show extensive diversification in age, genomic distribution, and developmental expression. Genome Res 32: 1408-1423, 2022.
11. Kohlrausch FB, Berteli TS, Wang F, Navarro PA and Keefe DL: Control of LINE-1 expression maintains genome integrity in germline and early embryo development. Reprod Sci 29: 328-340, 2022.
12. Lee HJ, Hou Y, Maeng JH, Shah NM, Chen Y, Lawson HA, Yang H, Yue F and Wang T: Epigenomic analysis reveals prevalent contribution of transposable elements to cis-regulatory elements, tissue-specific expression, and alternative promoters in zebrafish. Genome Res 32: 1424-1436, 2022.
13. Liang X, Hu Y, Feng S, Zhang S, Zhang Y and Sun C: Heavy chain (LvH) and light chain (LvL) of lipovitellin (Lv) of zebrafish can both bind to bacteria and enhance phagocytosis. Dev Comp Immunol 63: 47-55, 2016.
14. Romero S, Laino A, Molina G, Cunningham M and Garcia CF: Embryonic and post-embryonic development of the spider Polybetes pythagoricus (Sparassidae): A biochemical point of view. An Acad Bras Cienc 94: e20210159, 2022.
15. Li H and Zhang S: Functions of vitellogenin in eggs. Results Probl Cell Differ 63: 389-401, 2017.
16. Wang H, Sun W, Li Z, Wang X and Lv Z: Identification and characterization of two critical sequences in SV40PolyA that activate the green fluorescent protein reporter gene. Genet Mol Biol 34: 396-405, 2011.
17. Dang Y, Wang F and Liu C: Real-time PCR array to study the effects of chemicals on the growth hormone/insulin-like growth factors (GH/IGFs) axis of zebrafish embryos/larvae. Chemosphere 207: 365-376, 2018.
18. Dong M, Ding Y, Liu Y, Xu Z, Hong H, Sun H, Huang X, Yu X and Chen Q: Molecular insights of 2,6-dichlorobenzoquinone-induced cytotoxicity in zebrafish embryo: Activation of ROS-mediated cell cycle arrest and apoptosis. Environ Toxicol 38: 694-700, 2023.
19. Holbech H, Andersen L, Petersen GI, Korsgaard B, Pedersen KL and Bjerregaard P: Development of an ELISA for vitellogenin in whole body homogenate of zebrafish (Danio rerio). Comp Biochem Physiol C Toxicol Pharmacol 130: 119-131, 2001.
20. Li Z, Zhang S and Liu Q: Vitellogenin functions as a multivalent pattern recognition receptor with an opsonic activity. PLoS One 3: e1940, 2008.
21. Medina-Gali R, Belló-Pérez M, Ciordia S, Mena MC, Coll J, Novoa B, Ortega-Villaizán MDM and Perez L: Plasma proteomic analysis of zebrafish following spring viremia of carp virus infection. Fish Shellfish Immunol 86: 892-899, 2019.
22. Kielkopf CL, Bauer W and Urbatsch IL: Sodium dodecyl sulfate-polyacrylamide gel electrophoresis of proteins. Cold Spring Harb Protoc 2021: pdb. prot102228, 2021.
23. Stein A, Whitlock JP Jr and Bina M: Acidic polypeptides can assemble both histones and chromatin in vitro at physiological ionic strength. Proc Natl Acad Sci USA 76: 5000-5004, 1979.
24. Lusser A and Kadonaga JT: Strategies for the reconstitution of chromatin. Nat Methods 1: 19-26, 2004.
25. Athanikar JN, Badge RM and Moran JV: A YY1-binding site is required for accurate human LINE-1 transcription initiation. Nucleic Acids Res 32: 3846-3855, 2004.
26. You C, Ji D, Dai X and Wang Y: Effects of Tet-mediated oxidation products of 5-methylcytosine on DNA transcription in vitro and in mammalian cells. Sci Rep 4: 7052, 2014.
27. Purushothaman K, Das PP, Presslauer C, Lim TK, Johansen SD, Lin Q and Babiak I: Proteomics analysis of early developmental stages of zebrafish embryos. Int J Mol Sci 20: 6359, 2019.
28. Ji N, Wu CG, Wang XD, Song ZX, Wu PY, Liu X, Feng X, Zhang XM, Wang XF and Lv ZJ: Anti-aging effects of Alu antisense RNA on human fibroblast senescence through the MEK-ERK pathway mediated by KIF15. Curr Med Sci 43: 35-47, 2023.
29. Elshafie NO, Gribskov M, Lichti NI, Sayedahmed EE, Childress MO and Dos Santos AP: miRNome expression analysis in canine diffuse large B-cell lymphoma. Front Oncol 13: 1238613, 2023.
30. Guo M, Yang F, Zhu L, Wang L, Li Z, Qi Z, Fotopoulos V, Yu J and Zhou J: Loss of cold tolerance is conferred by absence of the WRKY34 promoter fragment during tomato evolution. Nat Commun 15: 6667, 2024.
31. Wei W, Cheng B, Yang X, Chu X, He D, Qin X, Zhang N, Zhao Y, Shi S, Cai Q, *et al*: Single-cell multiomics analysis reveals cell/tissue-specific associations in bipolar disorder. Transl Psychiatry 14: 323, 2024.
32. Langmead B and Salzberg SL: Fast gapped-read alignment with Bowtie 2. Nat Methods 9: 357-359, 2012.
33. Zhan Y, Yin A, Su X, Tang N, Zhang Z, Chen Y, Wang W and Wang J: Interpreting the molecular mechanisms of RBBP4/7 and their roles in human diseases (Review). Int J Mol Med 53: 48, 2024.
34. Farhana R, Lei R, Pham K, Derrien V, Cedeño J, Rodriquez V, Bernad S, Lima FF and Miksovska J: Globin X: A highly stable intrinsically hexacoordinate globin. J Inorg Biochem 236: 111976, 2022.
35. Li C, Tan XF, Lim TK, Lin Q and Gong Z: Comprehensive and quantitative proteomic analyses of zebrafish plasma reveals conserved protein profiles between genders and between zebrafish and human. Sci Rep 6: 24329, 2016.
36. Yilmaz O, Patinote A, Nguyen TV, Com E, Lavigne R, Pineau C, Sullivan CV and Bobe J: Scrambled eggs: Proteomic portraits and novel biomarkers of egg quality in zebrafish (Danio rerio). PLoS One 12: e0188084, 2017.
37. Moyano TC, Gutiérrez RA and Alvarez JM: Genomic footprinting analyses from DNase-seq data to construct gene regulatory networks. Methods Mol Biol 2328: 25-46, 2021.
38. Carmignac V, Barberet J, Iranzo J, Quéré R, Guilleman M, Bourc'his D and Fauque P: Effects of assisted reproductive technologies on transposon regulation in the mouse pre-implanted embryo. Hum Reprod 34: 612-622, 2019.
39. Navarro PA, Wang F, Pimentel R, Robinson LG Jr, Berteli TS and Keefe DL: Zidovudine inhibits telomere elongation, increases the transposable element LINE-1 copy number and compromises mouse embryo development. Mol Biol Rep 48: 7767-7773, 2021.
40. Han JS and Boeke JD: A highly active synthetic mammalian retrotransposon. Nature 429: 314-318, 2004.
41. Zhang P, Ludwig AK, Hastert FD, Rausch C, Lehmkuhl A, Hellmann I, Smets M, Leonhardt H and Cardoso MC: L1 retrotransposition is activated by Ten-eleven-translocation protein 1 and repressed by methyl-CpG binding proteins. Nucleus 8: 548-562, 2017.

42. Zhang S, Dong Y and Cui P: Vitellogenin is an immunocompetent molecule for mother and offspring in fish. Fish Shellfish Immunol 46: 710-715, 2015.
43. Veil M, Yampolsky LY, Grüning B and Onichtchouk D: Pou5f3, SoxB1, and Nanog remodel chromatin on high nucleosome affinity regions at zygotic genome activation. Genome Res 29: 383-395, 2019.
44. Wang J, Zhang X, Shan R, Ma S, Tian H, Wang W and Ru S: Lipovitellin as an antigen to improve the precision of sandwich ELISA for quantifying zebrafish (Danio rerio) vitellogenin. Comp Biochem Physiol C Toxicol Pharmacol 185-186: 87-93, 2016.
45. Thompson JR and Banaszak LJ: Lipid-protein interactions in lipovitellin. Biochemistry 41: 9398-9409, 2002.
46. Ramos KS, Bojang P and Bowers E: Role of long interspersed nuclear element-1 in the regulation of chromatin landscapes and genome dynamics. Exp Biol Med (Maywood) 246: 2082-2097, 2021.
47. Tian T, Wang L, Shen Y, Zhang B, Finnell RH and Ren A: Hypomethylation of GRHL3 gene is associated with the occurrence of neural tube defects. Epigenomics 10: 891-901, 2018.
48. Desai K, Spikings E and Zhang T: Effect of chilling on sox2, sox3 and sox19a gene expression in zebrafish (Danio rerio) embryos. Cryobiology 63: 96-103, 2011.
49. Fang F, Chen D, Basharat AR, Poulos W, Wang Q, Cibelli JB, Liu X and Sun L: Quantitative proteomics reveals the dynamic proteome landscape of zebrafish embryos during the maternal-to-zygotic transition. iScience 27: 109944, 2024.
50. Lindeman LC, Winata CL, Aanes H, Mathavan S, Alestrom P and Collas P: Chromatin states of developmentally-regulated genes revealed by DNA and histone methylation patterns in zebrafish embryos. Int J Dev Biol 54: 803-813, 2010.
51. Sokolova M and Vartiainen MK: Chromatin immunoprecipitation experiments from Drosophila ovaries. Methods Mol Biol 2626: 335-351, 2023.
52. Popchock AR, Larson JD, Dubrulle J, Asbury CL and Biggins S: Direct observation of coordinated assembly of individual native centromeric nucleosomes. EMBO J 42: e114534, 2023.
53. Pallarès-Albanell J, Ortega-Flores L, Senar-Serra T, Ruiz A, Abril JF, Rossello M and Almudi I: Gene regulatory dynamics during the development of a paleopteran insect, the mayfly Cloeon dipterum. bioRxiv: May 17, 2024 (Epub ahead of print).
54. Muto Y, Wilson PC, Ledru N, Wu H, Dimke H, Waikar SS and Humphreys BD: Single cell transcriptional and chromatin accessibility profiling redefine cellular heterogeneity in the adult human kidney. Nat Commun 12: 2190, 2021.
55. Jiang Z and Zhang B: On the role of transcription in positioning nucleosomes. PLoS Comput Biol 17: e1008556, 2021.
56. Zhao M, Wang Z, Yung S and Lu Q: Epigenetic dynamics in immunity and autoimmunity. Int J Biochem Cell Biol 67: 65-74, 2015.
57. Hocher A, Laursen SP, Radford P, Tyson J, Lambert C, Stevens KM, Montoya A, Shliaha PV, Picardeau M, Sockett RE, *et al*: Histones with an unconventional DNA-binding mode in vitro are major chromatin constituents in the bacterium Bdellovibrio bacteriovorus. Nat Microbiol 8: 2006-2019, 2023.
58. Wang SH, Liu L, Bao KY, Zhang YF, Wang WW, Du S, Jia NE, Suo S, Cai J, Guo JF and Lv G: EZH2 contributes to anoikis resistance and promotes epithelial ovarian cancer peritoneal metastasis by regulating m6A. Curr Med Sci 43: 794-802, 2023.
59. Guo H, Zhu P, Yan L, Li R, Hu B, Lian Y, Yan J, Ren X, Lin S, Li J, *et al*: The DNA methylation landscape of human early embryos. Nature 511: 606-610, 2014.